Journal of proteome research

ARTICLE

pubs.acs.org/jpr

Global Effects of Adriamycin Treatment on Mouse Splenic Protein Levels

Adam R. Evans,[†] Sumitra Miriyala,[‡] Daret K. St. Clair,[‡] D. Allan Butterfield,[§] and Renã A. S. Robinson*[,†]

[†]Department of Chemistry, University of Pittsburgh, Pittsburgh, Pennsylvania 15260, United States

[‡]Department of Toxicology, University of Kentucky, Lexington, Kentucky 40536, United States

[§]Department of Chemistry, Sanders-Brown Center on Aging, and Center of Membrane Sciences, University of Kentucky, Lexington, Kentucky 40506, United States

Supporting Information

ABSTRACT: Adriamycin (ADR) is a potent anticancer drug used to treat a variety of cancers. Patients treated with ADR have experienced side effects such as heart failure, cardiomyopathy, and "chemobrain", which have been correlated to changes in protein expression in the heart and brain. In order to better understand cellular responses that are disrupted following ADR treatment in immune tissues, this work focuses on spleen. Significantly reduced spleen sizes were found in ADR-treated mice. Global isotopic labeling of tryptic peptides and nanoflow reversed-phase liquid chromatography-tandem mass spectrometry (LC−MS/MS) were employed to determine differences in the relative abundances of proteins from ADR-treated mice relative to controls. Fifty-nine proteins of the 388 unique proteins identified showed statistically significant differences in expression levels following acute ADR treatment. Differentially expressed proteins are involved in processes such as cytoskeletal structural integrity, cellular signaling and transport, transcription and translation, immune response, and Ca^{2+} binding. These are the first studies to provide insight to the downstream effects of ADR treatment in a peripheral immune organ such as spleen using proteomics.

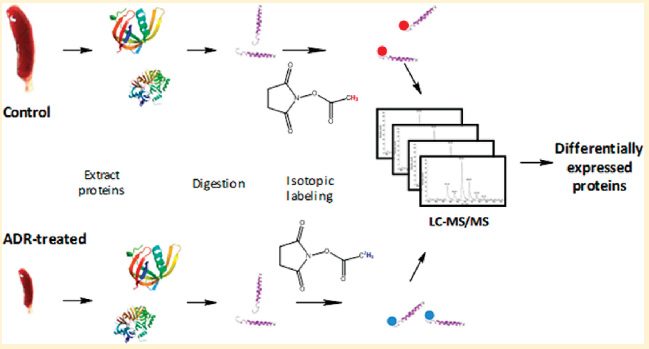

KEYWORDS: adriamycin, doxorubicin, spleen, proteomics, immunity, oxidative stress

INTRODUCTION

Adriamycin [(ADR), also known as doxorubicin] is an anthracycline drug used to treat both hemopoietic and a wide range of solid tumors in lung, breast, ovarian, prostate, and bladder cancers among others.[1,2] Although mechanisms of ADR drug action in noncancer tissues are not completely understood, there are two widely supported phenomenon. The first primary action involves the intercalation of DNA and inhibition of topoisomerase II enzymatic activity which results in the termination of DNA replication and transcription.[3,4] Clinically, ADR is very effective as an anticancer treatment; however, some patients can suffer from major side effects such as cardiomyopathy and heart failure,[5] dizziness, lack of concentration, and cognitive deficits characterized as "chemobrain".[6,7] In other cases, patients develop a resistance to ADR and treatment fails.[8]

The second primary action of ADR involves the generation of toxic free radical species. The structure of the drug contains a quinone which generates free radicals such as superoxide anion through a one-electron reduction of the quinone which is converted to a semiquinone; in the presence of oxygen, the semiquinone is converted back to the quinone.[9] This process of redox cycling results in large amounts of free radical species which become detrimental to nontargeted cells, in addition to cancerous cells, causing elevated levels of oxidative stress.[10] Oxidative stress can result in protein oxidation, DNA damage, and lipid peroxidation which disrupt cellular functions. Several reports have demonstrated that ADR leads to elevated oxidative stress in plasma,[11] brain,[12] heart,[13] cardiomyocytes,[14] liver,[15] testes,[16] and kidney.[17] The cytotoxicity of ADR also causes alterations to apoptotic pathways,[18] lipid membrane structure and function,[19] Ca^{2+} homeostasis,[20] and cellular arrest and differentiation.[21]

Proteomics methods have been employed to study the effects of ADR treatment in different cell lines and tissues, including brain,[12,22,23] plasma,[24] heart,[25] MCF-7 human breast cancer cells,[26] hepatoma cells,[27] Jurkat T cells,[28] Raji cells,[29] and thymus.[30] Proteomic studies of ADR-resistant cells lines[31] have been performed on K562/ADM cells,[32,33] K562/ADR cells,[34] DLKP cell lines,[35] and MCF-7/ADR cells.[36−38] The most commonly used proteomic strategy relies on two-dimensional (2D) polyacrylamide gel electrophoresis (PAGE) combined with in-gel digestion and mass spectrometry (MS) analysis of excised protein spots. Other approaches have used isotopic labeling strategies such as stable isotope labeling by amino acids in cell

Received: August 18, 2011
Published: November 22, 2011

culture (SILAC)[27,28,39] and ^{18}O labeling[36] with liquid chromatography (LC)-tandem mass spectrometry (MS/MS) in order to detect proteins that change as a result of ADR treatment or resistance.

To date, no proteomics studies of spleen tissue from ADR-treated mice have been reported. It has been shown, however, that cellular populations in spleen tissue undergo substantial changes after ADR treatment which may have global effects on immunity in ADR-treated patients.[40] Herein is the first report that has examined the effects of ADR treatment on protein expression in spleen. The proteomics methods employed involved a combination of a global internal standard technology (GIST) post-digestion isotopic labeling approach[41] with nanoflow liquid chromatography (LC)-tandem MS (MS/MS) to quantify relative differences in splenic protein expression in control and ADR-treated mice.

EXPERIMENTAL SECTION

Animal Housing and Treatment

Approximately 3 month old male B6C3 mice were housed at the University of Kentucky Central Animal Facility with 12 h light/12 h dark cycle. Animals were fed standard Purina rodent chow ad libitum. The animal protocol was approved by the University of Kentucky Animal Care and Use Committee. Animals used in these studies were the same as those previously reported.[30] Mice were divided into two groups and injected with either saline (hereafter referred to as control mice) or adriamycin (25 mg/kg body weight; hereafter referred to as ADR-treated mice). Spleen tissue was harvested 72 h post injection from saline-perfused mice. For these studies, $N = 5$ was used for each treatment group.

Spleen Homogenization

Spleen tissues were homogenized in a ice-cold phosphate buffer saline (PBS) solution containing 8 M urea with 100 passes of a Wheaton homogenizer. Homogenate solution was collected, sonicated, and centrifuged at 13 000 rpm for 10 min (4 °C). Supernatants were collected, and protein concentrations determined using the BCA assay according to the manufacturer's instructions (Pierce Thermo; Rockford, IL). Samples were stored at −80 °C until further use.

Protein Digestion

For individual samples, 100 μg of spleen protein was spiked with 1 μg of bovine β-lactoglobulin (Sigma Aldrich; St. Louis, MO) and subject to tryptic digestion as follows: 0.25 M dithiothreitol (Thermo Fisher; Pittsburgh, PA) was added in a 1:40 protein/reagent molar excess and incubated at 37 °C for 2 h. Then 0.25 M iodoacetamine (Acros Organics; Morris Plains, NJ) was added in a 1:80 protein/reagent molar excess and incubated at 0 °C for 2 h in the dark followed by the addition of 0.25 M L-cysteine in a 1:40 protein/reagent molar excess at room temperature for 30 min. Tris buffer solution (0.2 M Tris, 10 mM $CaCl_2$, pH 8.0) was added to reduce the urea concentration to 2 M. TPCK-treated trypsin from bovine pancreas (Sigma Aldrich) was added to each sample in a 2% w/w enzyme to that of protein ratio and incubated at 37 °C for 24 h. Samples were flash-frozen with liquid nitrogen and cleaned using Waters Oasis HLB C18 cartridges.

Synthesis of *N*-Acetoxy-H_3-succinimide and *N*-Acetoxy-$^2H_3$-succinimide

The procedure for synthesis of *N*-acetoxy-H_3-succinimide and *N*-acetoxy-$^2H_3$-succinimide is described elsewhere.[42] Briefly, 1.9478 g of *N*-hydroxysuccinimide (NHS, Sigma Aldrich) was added to 4.8 mL of >99% acetic anhydride (Sigma Aldrich) or 1.9451 g of NHS was added to 4.4 mL of 99% atom $^2H_6$-acetic anhydride (Sigma Aldrich). Both reactions occurred at room temperature for 15 h under nitrogen. White crystal products were collected, washed thoroughly with hexane, and dried under vacuum. Product purity was confirmed with NMR analysis (>95% purity).

Isotopic Labeling of Peptides

Stock solutions (0.25 M) of *N*-acetoxy-H_3-succinimide and *N*-acetoxy-$^2H_3$-succinimide were prepared in 50 mM phosphate buffer (pH = 7.5). Tryptic peptide samples (1 mg·mL^{-1}) were reconstituted in 50 mM phosphate buffer and reacted with 100 molar excess of the *N*-acetoxy-H_3-succinimide (light) and *N*-acetoxy-$^2H_3$-succinimide (heavy) for control and ADR-treated mice, respectively. Reactions occurred at room temperature for 5 h under constant stirring. Control and ADR-treated samples were pooled and treated with excess 0.25 M hydroxylamine hydrochloride (Sigma Aldrich) and adjusted to pH 10. After 20 min at room temperature, the samples were adjusted to pH 7 and were cleaned, dried, and stored at −80 °C.

LC−MS/MS

Isotopically labeled peptide samples were reconstituted in formic acid solution (0.1% in water) to a concentration of 0.5 μg·μL^{-1} and injected onto a trapping column (2 cm ×100 μm i.d.) packed with 200 Å C_{18} material (Miczhrom Bioresources Inc.; Auburn, Ca) using an autosampler on a nanoflow Eksigent 2D LC system. Buffers A and B were composed of water/acetonitrile (97:3) and acetonitrile, respectively, each with 0.1% formic acid. Samples were washed with buffer A and eluted onto an analytical column (13.2 cm × 75 μm i.d.) packed with 100 Å C_{18} material (Michrom Bioresources Inc.). Gradient elution was performed as follows (%A/%B): 90:10 for 2 min, ramp to 85:15 over 4 min, hold for 4 min, ramp to 70:30 over 120 min, ramp to 40:60 over 30 min, ramp to 20:80 over 5 min, hold for 10 min followed by column re-equilibration. Eluted peptides were detected on an LTQ-Orbitrap Velos MS using data-dependent acquisition with the following parameters: full FT parent scan at 60 000 resolution over the m/z range of 300−1800, positive ion mode, the top 6 most intense ions were selected for CID fragmentation (35% collision energy, 10 ms activation time, 5000 minimum ion count threshold) and mass analyzed using the LTQ. Each pooled isotopically labeled sample ($N = 5$) was analyzed with three technical LC−MS/MS replicates.

Database Searching and Analysis

RAW files were searched against the mouse International Protein Index (IPI) database (56 957 total sequences on 4/26/2010) using the SEQUEST algorithm embedded in Proteome Discoverer 1.2 software (Thermo). The .fasta sequence for bovine β-lactoglobulin (National Center for Biotechnology Information Accession Number: gi4388846) was manually added to the database. Search parameters included: precursor mass tolerance of 15 ppm, fragmentation tolerance of 1.0 Da, dynamic modifications of light and heavy acetyl groups on lysine residues and the N-terminus and oxidation of methionine, and a static modification of carbamidomethyl on cysteine. All files were searched against a decoy database with false discovery rates set at $p < 0.05$ and $p < 0.01$ so that only medium and high confidence peptides, respectively, were used for further analysis. Proteome

Discoverer 1.2 provided peak intensity and area information for light and heavy labeled peptides and protein ratio calculations.

Statistics for Differentially Expressed Proteins

The search results were treated as follows in order to generate a confident and conservative list of differentially expressed proteins. After calculation of protein ratios, the protein list was filtered to include only proteins that were detected in a minimum of any six LC−MS/MS analyses. One-way ANOVA ($p < 0.05$) was carried out in Origin 8.0 to assess statistical differences in the ADR/control (CTR) ratios across biological ($N = 5$) and technical ($N = 3$) replicates for each protein. Proteins were considered to be significantly differentially expressed if the following two criteria were met: (1) a calculated F score < the tabulated F score and (2) a ADR/CTR or CTR/ADR ratio > 1.5.

Table 1. Masses of spleen Tissues Collected from Control and Adr Treated Mice

animal	control (g)	ADR (g)
1	0.0814	0.0297
2	0.0909	0.0346
3	0.0859	0.0378
4	0.115	0.0269
5	0.0840	0.0278
avg. ± SD	0.0914 ± 0.0135	0.0314 ± 0.0047

Western Blot Validation

Protein samples (50 μg) were denatured in an appropriate sample buffer and electrophoretically separated on a Criterion TGX gel (Biorad Laboratories; Hercules, CA) at 250 V. Protein from the gel was transferred onto a nitrocellulose membrane paper using a Fast-Transfer Blot System (Biorad). Blots were washed three times in Wash blot. BSA blocking solution was added to the membrane and incubated on a rocker for 1 h. A 1:1000 dilution of rabbit polyclonal antiannexin A2 primary antibody (Sigma Aldrich) and 1:2000 dilution of rabbit polyclonal antiactin primary antibody (Sigma Aldrich) was added and incubated at 4 °C overnight. The blot was rinsed and incubated with a 1:8000 dilution of antirabbit IgG alkaline phosphatase secondary antibody (Sigma Aldrich) for 1 h on a rocker. The blot was rinsed and colorometrically developed. The dried blot was scanned using a Canon scanner, saved as a .TIFF file, and densitometry analyses carried out with Scion Image Software.

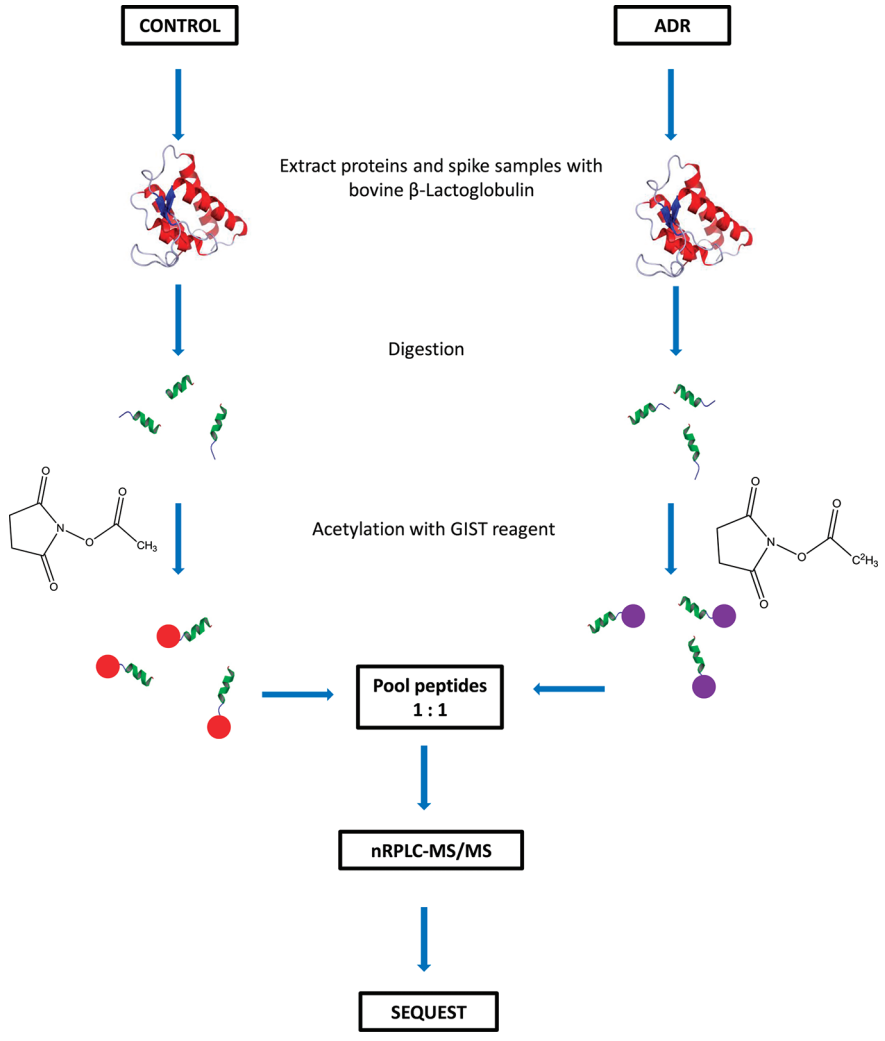

Figure 1. Schematic diagram of the proteomics workflow involving internal standard spiking, GIST labeling, and nanoflow RP LC-MS/MS to determine differences in relative protein expression after ADR treatment in mouse spleen.

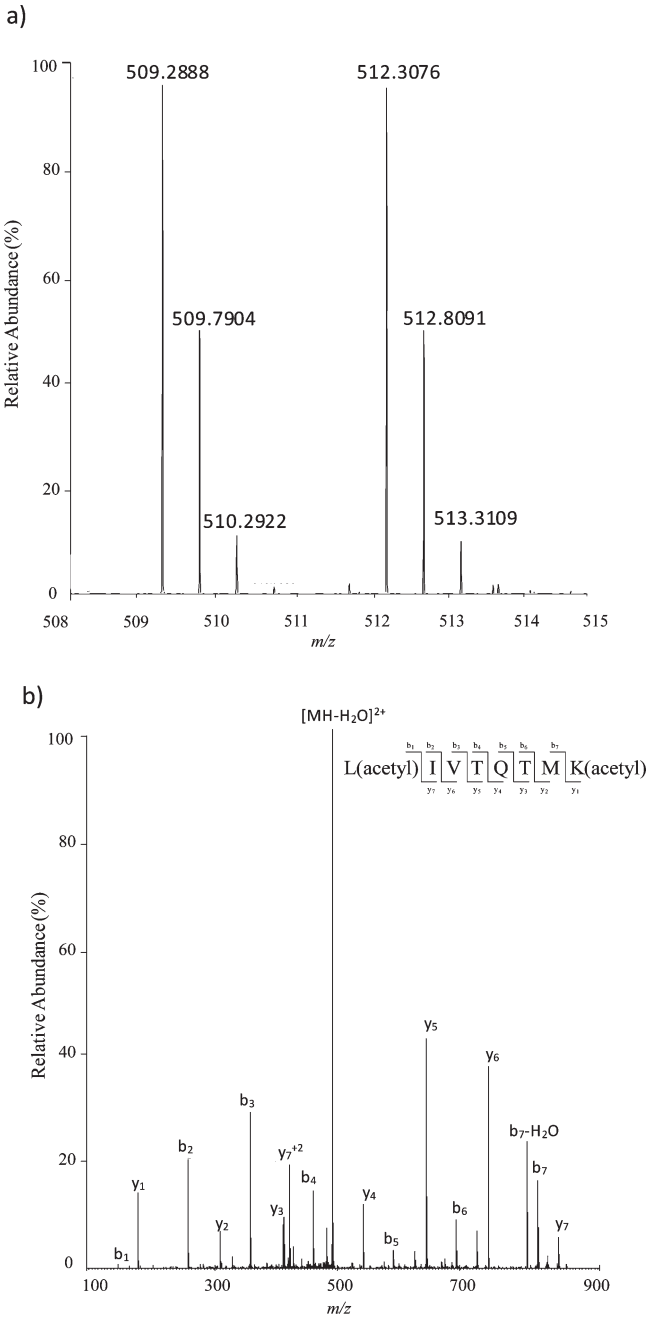

Figure 2. Example mass spectra (a) of a peak pair that eluted at t_r 80.8 min with m/z 509.2888 and 512.3076 for the light and heavy labeled peaks, respectively, and (b) of the CID generated fragments obtained upon isolation of the light labeled peak at m/z 509.2888. The peptide assigned in the figure belongs to β-lactoglobulin.

RESULTS

Effects of ADR Treatment on Spleen Tissue

In order to better understand the effects that ADR treatment has on spleen tissue, we initially began by measuring spleen weights. The ADR-treated mice used in these studies exhibited an ~11% decrease in body weight and an ~68% decrease in thymus weight.[30] Additionally, this work reports an ~66% loss in spleen weight of ADR-treated mice relative to controls (Table 1). Because lower body weight and thymus size are correlated with lower numbers of lymphocytes,[30] we hypothesize that there is also a lower number of splenic lymphocytes based on smaller spleen sizes in ADR-treated mice.

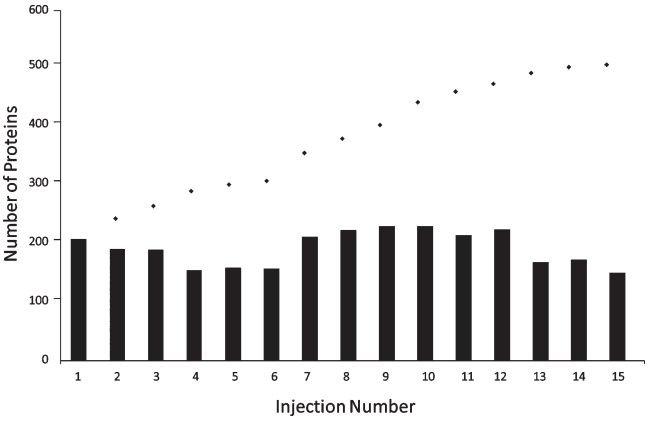

Figure 3. Bar graph of the total number of proteins identified in individual LC−MS/MS analyses [bars] and the total number of newly assigned proteins identified with each consecutive experiment [◆]. The values shown include redundant protein assignments that arise due to isoforms, etc.

GIST Proteomics Workflow

The semiquantitative proteomics workflow, shown in Figure 1, was used to determine differences in protein expression after ADR treatment as follows. Protein samples extracted from homogenized spleen tissue of control and ADR-treated mice were spiked with an internal protein standard (i.e., bovine β-lactoglobulin) prior to trypsin digestion. Tryptic peptide samples from control and ADR-treated mice were isotopically labeled with either a light or heavy GIST reagent, respectively, and pooled in a 1:1 ratio. Isotopically labeled peptide mixtures ($N = 5$ for biological replicates) were analyzed with triplicate nanoflow LC−MS/MS experiments using a LTQ-Orbitrap Velos MS. Identified proteins were filtered (as discussed above) in order to generate a list of differentially expressed proteins.

Internal Standard Normalization

Figure 2a shows an example parent mass spectrum obtained for a doubly charged peptide pair at m/z 509.2888 and 512.3076 that eluted from the column at $t_r = 80.8$ min. The observed mass shift of 6 Da between the light and heavy labeled peptide peaks indicates that the peptide contains the addition of two acetylations to the peptide sequence. The CID MS/MS spectrum for the light labeled peptide is shown in Figure 2b displaying a consecutive series of b- and y-fragment ions. The CID MS/MS spectrum for the heavy labeled peptide is similar (data not shown). This peptide pair has been assigned as the $[(\text{Acetyl})\text{LIVQTMK}(\text{Acetyl})+2\text{H}]^{2+}$ peptide of β-lactoglobulin. The ratio of heavy/light labeled peptides for the internal standard should be unity as 1 μg of β-lactoglobulin was spiked into protein extracts of both control and ADR-treated spleen samples. The measured ratio for heavy/light labeled peaks shown in Figure 2a is 1.0 based on peak areas which agree with the expected values. The ratio values for other tryptic peptides of β-lactoglobulin are similar and an average protein ratio value of 0.98 ± 0.10 is observed across all 15 injected samples. β-lactoglobuin ratio values within each technical replicate were used to normalize ratio values of mouse splenic proteins.

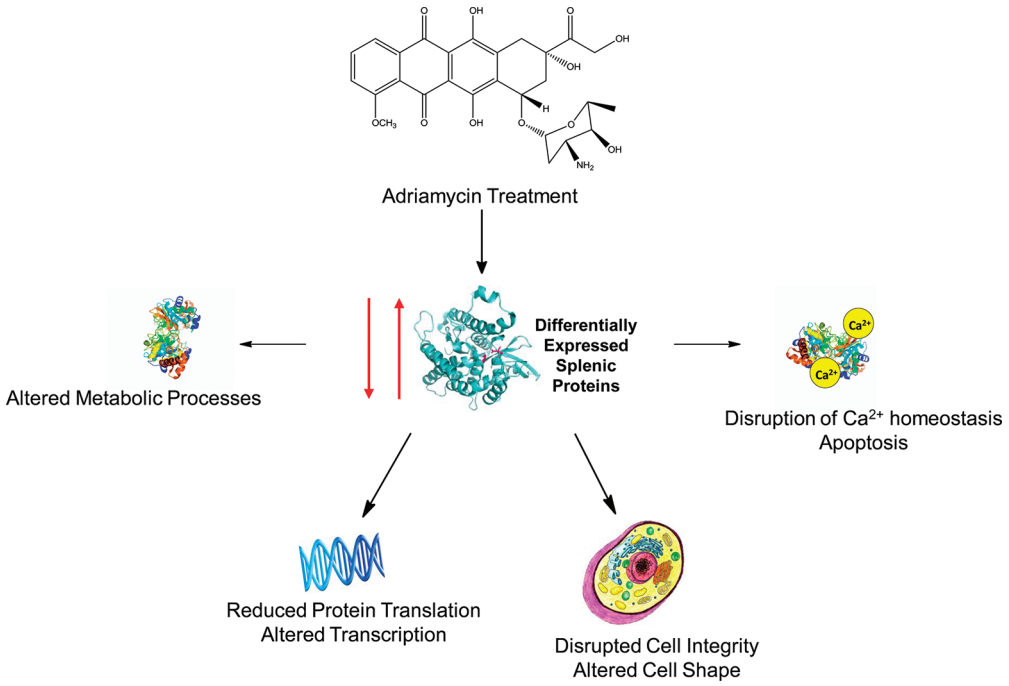

Figure 4. Illustrative depiction of differentially expressed splenic proteins (pathways) that are affected from ADR-treatment.

As discussed above, each isotopically labeled peptide mixture was subject to triplicate LC−MS/MS analyses. Figure 3 shows a bar graph of the total number of proteins identified in each individual analysis. The average number of proteins detected in a single injection is 189 ± 29. The total number of proteins identified increases with each new sample injection such that, after accounting for redundant entries, we identified a total of 388 unique proteins across the 15 injections. This accounts for a total of 70 033 spectral peptide counts. A list of proteins, including peptide and quantitative ratio information, is included in Supporting Information Table SI.

Differentially Expressed Proteins in ADR-Treated Mice

Using a conservative set of criteria (see Experimental), 59 proteins were assessed as differentially expressed in ADR-treated mice (Table 2). These proteins are involved in processes such as cell signaling, protein translation, defense response, metabolism, Ca^{2+} binding and apoptosis, and structural stability. In total, 37 proteins are upregulated (ADR/CTR > 1.5) and 21 proteins are downregulated (CTR/ADR > 1.5). Most of the upregulated proteins and all of the downregulated proteins change by a factor of 1.5−4.0. Four upregulated proteins (i.e., complement C3 protein, tropomyosin 2, peptidyl-*cis/trans*-isomerase, and hemopexin) were expressed by a factor of >4 in spleen tissue as a result of ADR treatment. Figure 4 shows a graphical illustration of the major pathways affected by ADR treatment which we discuss below.

MS/MS and Western Analysis of Annexin A2

Figure 5a shows an example MS/MS spectrum for a doubly charged peptide pair at m/z 792.9354 and 794.4449. The isotopically labeled peaks have a ADR/CTR ratio of 2.0, indicating the upregulation of this species in ADR-treated mice. The MS/MS spectrum in Figure 5b shows fragment ions that correspond to the peptide sequence $[(\text{Acetyl})\text{GVDEVTIVNIL-TNR+2H}]^{2+}$ that belongs to the protein annexin A2. Annexin A2 has an average ADR/CTR ratio of 2.5 ± 0.4 as measured across 11 injections (Table 2). Western validation was carried out in order to confirm protein changes measured with our proteomics workflow for annexin A2. Figure 6 shows an example Western blot obtained for control and ADR-treated splenic proteins for annexin A2 and actin (loading control). A 50% increase in annexin A2 levels is observed in ADR-treated mice supporting upregulation of this protein which is consistent with proteomics results (Figure 5).

DISCUSSION

This work reports the first investigation of the effects of ADR treatment on splenic protein levels in mice. The spleen is an important organ to study as it is involved in innate and adaptive immunity and helps to regulate immune homeostasis.[43] The spleen consists of lymphocytes such as T-cells, B-cells, and macrophages with functions that include blood filtering, iron recycling, pathogen response, and immune induction, activation, and proliferation.[43] These functions are critical for normal conditions and even more so in diseased states such as cancer. Smaller spleen weight, as measured in this work (Table 1), is consistent with other reports of reduced body weight and spleen size in ADR-treated mice[30,44−46] and supports the notion that altered cell differentiation[21] as well as decreased lymphocyte proliferation[44,47]occurs with ADR treatment. Reduced spleen size is also reflective of lower numbers of lymphocytes, which occurs with aging,[48] and could result in a weakened immune response in ADR-treated patients.

Following acute ADR treatment in mice, 59 splenic proteins were differentially expressed (Table 2). Below is a discussion of these proteins which are involved in a number of biological processes such as Ca^{2+} binding and apoptosis, DNA transcription and repair, cellular signaling, redox maintenance, metabolism, immune/defense response, and structural maintenance (Figure 4).

dx.doi.org/10.1021/pr200798g |*J. Proteome Res.* 2012, 11, 1054–1064

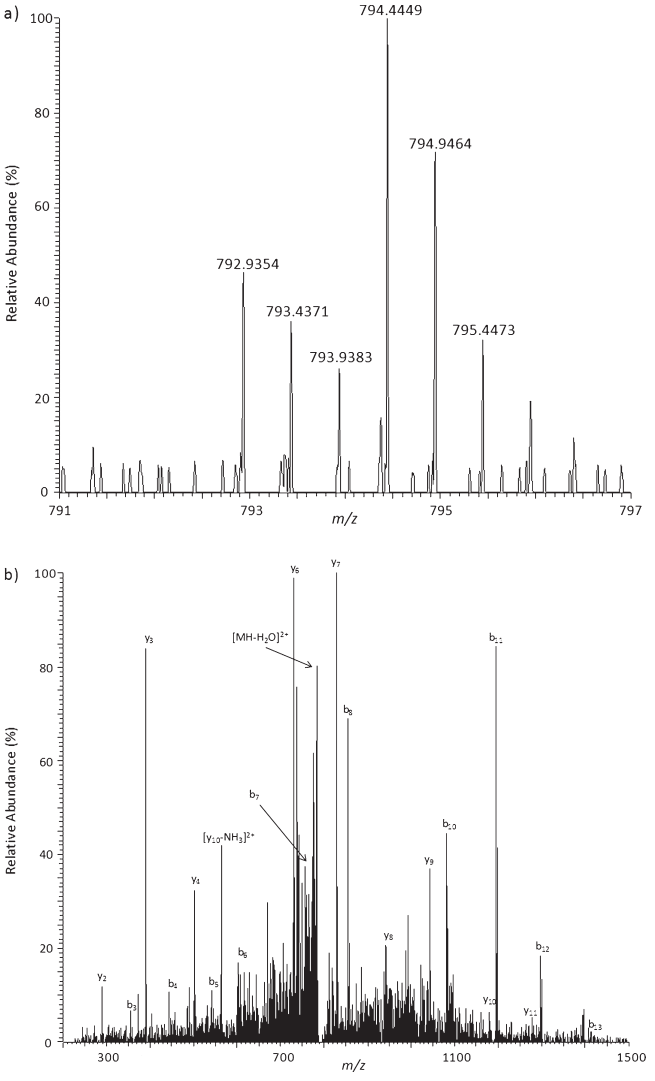

Figure 5. Example mass spectra (a) of a peak pair that eluted at t_r 117.5 min with m/z 792.9354 and 794.4449 for the light and heavy labeled peaks, respectively, and (b) of the CID generated fragments obtained upon isolation of the light labeled peak at m/z 792.9354. The peptide assigned as $[(\text{Acetyl})\text{GVDEVTIVNILNR}+2\text{H}]^{2+}$ belongs to the annexin A2 protein.

Ca^{2+} Binding/Apoptosis

Proteins involved in Ca^{2+}-binding, apoptosis, and chaperone activity were upregulated in ADR-treated mice. Annexins 2 and 5 belong to a class of Ca^{2+}-dependent membrane binding proteins. Annexin binds to both free Ca^{2+} and the phospholipids of the membrane structure[49] and may be a key moderator of apoptosis. Annexin A2 has been reported as upregulated in ADR resistant cells[32,50] suggesting its importance for chemoresistance. Annexin A5 has been found to inhibit apoptosis of phagocytes.[51] Upregulation of annexin A5 in ADR-treated mice is consistent with upregulation in the thymus,[30] ADR-treated HepG2 cells,[27] and in MCF-7/ADR resistant cells.[37,39]

Calreticulin, is a Ca^{2+} binding chaperone protein that is localized to the endoplasmic reticulum. Although calreticulin has a number of biological functions its primary roles involve modulation of Ca^{2+} homeostasis and molecular chaperone activity. Upregulation of calreticulin can lead to elevated levels of free Ca^{2+} that is housed in intracellular stores.[52] Additionally this protein is localized to the cell surface and is critical for initiating immune response.[53] In ADR-treated cells calreticulin migrates from the ER and localizes to the surface of preapoptotic and cancerous cells which will undergo clearance by lymphocytes.[54] Calmodulin is another Ca^{2+} binding protein which is involved in Ca^{2+} homeostasis, cellular growth, proliferation, and transport processes and has been implicated in chemoresistance of cancer therapies.[55] Ca^{2+} ion flux is important in modulating cell death in the immune system,[56] thus overexpression of Ca^{2+} binding proteins observed in ADR-treated mice could alter free Ca^{2+} levels and lead to irreversible cell injury and death.

Transcription and Translation

Several transcriptional and translational-related proteins were down regulated in ADR-treated mice. Histone proteins oligomerize to form the nucleosome, which is the core component of chromatin and help to recruit proteins to DNA. Nucleolin is a histone chaperone protein that is found on the surface of cancerous cells.[57] Down-regulation of nucleolin and histones H1.5 and H3.2 may be directly related with ADRs mechanistic action of DNA intercalation and inhibition of topoisomerase II which results in disrupted transcription. Other histone proteins have been reported as upregulated in human Jurkat T-cells treated with ADR.[28] It is not clear why there are differences in histone expression between these studies but it is implied that transcription is affected by ADR treatment.

The 40S ribosomal proteins SA, S3, and S14 were downregulated in ADR-treated mice which is consistent with studies in ADR-treated Jurkat T-cells.[28] Heterogeneous nuclear ribonucleoproteins (HNRP) in this work differed in expression levels. For example, HNRP A1 is down regulated where as HNRP F is upregulated (Table 2) in ADR-treated mice. In Raji cells treated with ADR, HNRP C1/C2 was downregulated, whereas in ADR resistant cells HNRP D is upregulated.[32] Polyadenylate-binding protein 1, another protein involved in protein translation, is down regulated in these studies. Overall, it appears that ADR treatment reduces protein translational activity which may be related with oxidative damage and altered transcription.

Cytoskeletal/Structural Proteins

Proteins involved in integrity of the cytoskeleton or other structures represent the largest group of differentially expressed proteins in ADR-treated mice. Cytoskeletal proteins have been implicated as potential targets for chemotherapeutic treatments in cancer.[58] Cytoskeletal/structurally related proteins in these studies were all found to be upregulated, with the exception of F-acting-capping protein which is down regulated in ADR-treated mice. Up-regulation of filamin, tropomyosin, spectrin, and tubulin is consistent with studies in ADR-treated HepG2 cells.[27] Vimentin is upregulated in these studies and in ADR-treated human Jurkat T cells[28]but has also been reported as downregulated in ADR-treated Raji cells.[29]

Tubulin proteins are the base unit of microtubules in the cell which are needed for cellular transport and structural integrity. Both α- and β-tubulin were upregulated in the thymus of ADR-treated mice[30] which is consistent with these results. However, β-tubulin has also been observed to be downregulated following ADR treatment.[27] α-Actinin is a ubiquitously expressed cytoskeletal protein that is compromised of an actin-binding domain, acalmodulin-like domain, and a calponin-homology domain.[59] Actinin belongs to a family of F-actin cross-linking proteins that also includes spectrin. α-actinin-1 and -4 are found in non-muscle tissues and are necessary for T-cell migration and activation.[59]

The proteins described above as well as transgelin, transgelin-2, and dihydropyrimidinase-related protein 2 detected in these studies, each has a key role for normal maintenance of the cytoskeletal structure. Upregulation of cytoskeletal proteins following ADR treatment could occur due to a compensatory

Table 2. List of Differentially Expressed Proteins in ADR-Treated Mice

accession[b]	protein name	ADR/CTR ± SE[c]	total injection number[d]	function
		upregulated		
00130589.8	superoxide dismutase [Cu−Zn]	1.5 ± 0.3	14	antioxidant
00317309.5	annexin A5	2.0 ± 0.3	15	Ca+2 binding/apoptosis
00885292.1[a]	annexin A2	2.5 ± 0.4	11	Ca2+ binding
00761696.2	calmodulin	3.5 ± 2.1	6	Ca2+ binding/apoptosis
00123639.1	calreticulin	1.9 ± 0.7	11	Ca2+ binding/chaperone
00319992.1	78 kDa glucose-regulated protein	1.6 ± 0.3	12	Ca2+ chaperone
00128484.1	hemopexin	18 ± 7.6	6	immune response
00323624.3	complement C3	5.5 ± 1.3	10	immune response
00406302.2[a]	alpha-1-antitrypsin 1−1	2.3 ± 0.4	11	immune response
00118413.2[a]	thrombospondin 1	1.8 ± 0.4	10	immune response
00131830.1	serine protease inhibitor A3K	3.8 ± 1.2	6	metabolism
00831033.1	phospholipase D4	3.1 ± 1.2	6	metabolism
00928204.1[a]	sulfated glycoprotein 1 preproprotein	3.1 ± 0.7	11	metabolism
00466919.7	6-phosphogluconate dehydrogenase, decarboxylating	2.8 ± 1.8	12	metabolism
00221402.7	fructose-bisphosphate aldolase A	2.5 ± 1.5	13	metabolism
00649586.1[a]	nucleoside diphosphate kinase	1.8 ± 0.6	8	metabolism
00111218.1	aldehyde dehydrogenase, mitochondrial	1.6 ± 0.1	11	metabolism
00135686.2	peptidyl-prolyl cis−trans isomerase B	6.2 ± 3.1	8	signaling
00894769.1	Parkinson disease (Autosomal recessive, early onset) 7	1.7 ± 0.7	10	signaling
00118899.1	alpha-actinin-4	3.3 ± 1.3	15	structure
00380436.1	alpha-actinin-1	2.2 ± 0.6	15	structure
00114375.2	dihydropyrimidinase-related protein 2	2.3 ± 0.3	10	structure
00874728.1	Isoform 2 of tropomyosin beta chain	5.9 ± 2.5	9	structure
00421223.3	tropomyosin alpha-4 chain	3.6 ± 1.0	14	structure
00405227.3	vinculin	3.2 ± 0.5	15	structure
00830701.1	37 kDa protein	3.0 ± 0.6	6	structure
00348094.4	tubulin, beta 1	2.1 ± 0.7	6	structure
00131376[a]	spectrin beta chain, erythrocyte	1.9 ± 0.7	7	structure
00465786.3	talin-1	1.9 ± 0.2	15	structure
00227299.6	vimentin	1.8 ± 0.2	15	structure
00130102.4	desmin	2.4 ± 0.3	11	structure
00226515.5	transgelin	2.3 ± 0.3	11	structure
00125778.4	transgelin-2	1.9 ± 0.3	14	structure
00664643.2[a]	filamin, alpha	1.8 ± 0.2	15	structure
00226073.2[a]	Heterogeneous nuclear ribonucleoprotein F	1.6 ± 0.7	6	translation
00109044.8[a]	myosin	3.1 ± 1.5	11	transport
00938530.1	myosin-11 isoform 1	1.6 ± 0.3	14	transport
00123181.4	myosin-9	1.6 ± 0.2	15	transport
		downregulated		
00320217.9	T-complex protein 1 subunit beta	0.64 ± 0.06	9	chaperone
00755843.1[a]	SET translocation	0.50 ± 0.11	6	chaperone
00136906.1	macrophage-capping protein	0.43 ± 0.10	9	immune response/ structure
00112719.1	delta-aminolevulinic acid dehydratase	0.44 ± 0.19	9	metabolism
00420363.2	probable ATP-dependent RNA helicase DDX5	0.50 ± 0.09	7	metabolism
00665513.3	putative uncharacterized protein Gm6636	0.49 ± 0.19	6	metabolism
00754464.1[a]	GTPase IMAP family member 4	0.58 ± 0.33	6	metabolism
00223757.4	aldose reductase	0.52 ± 0.16	6	metabolism
00113996.7	flavin reductase	0.37 ± 0.17	7	redox
00127358.1	SH3 domain-binding glutamic acid-rich-like protein 3	0.65 ± 0.11	7	redox
00462291.5	high mobility group protein B2	0.26 ± 0.05	6	signaling
00656269.1	14−3−3 protein theta	0.66 ± 0.17	8	signaling

dx.doi.org/10.1021/pr200798g |J. Proteome Res. 2012, 11, 1054–1064

Table 2. Continued

		downregulated		
00330063.6[a]	F-actin-capping protein subunit alpha	0.65 ± 0.09	6	structure
00317794.5	nucleolin	0.39 ± 0.06	8	transcription
00230133.5	histone H1.5	0.41 ± 0.05	10	transcription
00282848.1	histone H3.2	0.66 ± 0.08	10	transcription
00124287.1	polyadenylate-binding protein 1	0.59 ± 0.10	6	translation
00123604.4	40S ribosomal protein SA	0.62 ± 0.32	7	translation
00134599.1	40S ribosomal protein S3	0.25 ± 0.08	8	translation
00322562.5	40S ribosomal protein S14	0.62 ± 0.13	6	translation
00817004.1	heterogeneous nuclear ribonucleoprotein A1	0.53 ± 0.11	6	translation

[a] Indicates a protein sequence that was returned in the search results with redundant identifications due to protein isoforms that could not be distinguished based on peptides observed. [b] Accession numbers reported are taken from the International Protein Index mouse database. [c] Values represent the average ADR/CTR value ± standard error, whereby $6 < N < 15$ (see Experimental Section for details) depending on the number of biological and technical replicates in which the protein (peptides) were observed. [d] Total count of proteins identifications across all experiments (injections). Six $< N < 15$.

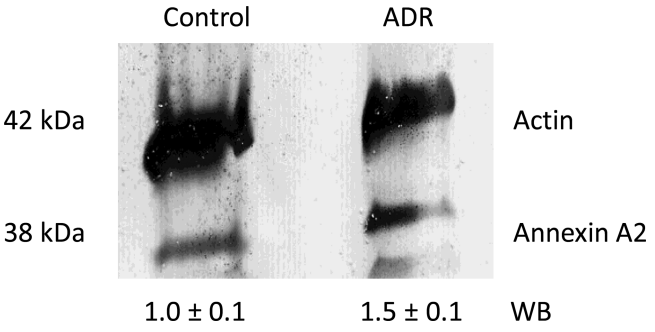

Figure 6. Example Western blot image of annexin A2 and actin (loading control) protein expression. The percent annexin A2 in control and ADR-treated mice obtained after normalization of annexin A2 levels to actin levels are listed underneath the image, $N = 3$.

mechanism to maintain structural stability. In addition to detrimental effects caused by cancerous cells, chemotherapeutic compounds (e.g., ADR) have been suggested to be a major cause of disruption of cytoskeletal proteins.[60] Consequences of disrupted cytoskeletal integrity include alterations to cell shape, growth, and transport which may lead to cell destruction and failure.

Chaperone/Immune and Defense Response/Antioxidant

Differential regulation of proteins involved in cellular defense processes indicates that cells are under attack or there is cellular dyshomeostasis, particularly in these studies as a result of ADR treatment. Glucose-regulated 78 kDa (GRP78) protein belongs to the class of heat shock 70 proteins, which serve as molecular chaperones. GRP78 is endoplasmic reticulum resident and involved in misfolded protein response. Other functions of GRP78 include Ca^{2+} homeostasis, apopotosis, and cellular signaling related with cancer cell proliferation and survival.[61] GRP78 overexpression is associated with a number of cancers and may be indicative of cellular stress or favorable survival outcomes due to the removal of cancerous cells.[61] Upregulation of GRP78 in these studies may suggest that ADR treatment provides cells with additional defenses against misfolded proteins that are likely to occur in cancer patients. Down regulation of T-complex protein 1-a cytosolic chaperone protein[62]- suggests that there is an imbalance in the overall cellular chaperone machinery in the presence of ADR.

Immune response proteins: complement C3, α-1-antitrypsin 1-1, and thrombospondin 1 were upregulated in ADR-treated mice. Thrombospondin 1 inhibits tumor cell progression and angiogenesis and has been investigated as a potential target for cancer therapy.[63] Due to the multifunctional roles of thrombospondin 1, it is possible that upregulation of this protein following ADR treatment results in reduced tumor growth in normal and cancerous cells. Complement C3 is directly involved in the complement system that is a part of the innate immune response. α-1 antitrypsin 1, a proteinase inhibitor, is also involved in immune response by protecting cells in inflammatory conditions. Hemopexin, is a scavenger of free heme, that is used to transport molecular oxygen. It belongs to the acute-phase proteins which can be activated in the immune system under inflammatory conditions and is sometimes localized to the surface of macrophages in spleen for receptor binding.[64] ADR treatment, based on upregulation of these splenic proteins, may help to increase immune response by initiating compensatory inflammation mechanisms.

Superoxide dismutase (SOD) is an endogenous antioxidant defense enzyme that eliminates superoxide anion through catalyzing the dismutation of superoxide anion to oxygen and hydrogen peroxide. Manganese SOD has been heavily implicated in cancer,[65] however we detected upregulation of Cu−Zn SOD (or SOD1) in ADR-treated mice. St. Clair et al. demonstrated that an overexpression of SOD2 in heart tissue helps protect the heart from oxidative damage and ADR cardiotoxicity.[66] Due to the antioxidant nature of SOD, upregulation of this enzyme may be in result to the free radicals generated from ADR redox recycling and thus serves to protect cells from oxidative damage.

Metabolism

Metabolic proteins in these studies had various expression in response to ADR treatment (Table 2). Serine protease inhibitor A3K, isoform 2 of phospholipase D4, sulfated glycoprotein 1 preprotein, 6-phosphogluconate dehydrogenase, fructose-bisphosphate aldolase A, nucleoside diphosphate kinase, and aldehyde dehydrogenase were upregulated in ADR-treatment mice, whereas δ-aminolevulinic acid dehydratase, probable ATP-dependent RNA helicase DDX5, GTPase IMAP family member 4, aldose reductase, and flavin reductase were downregulated. Alterations to metabolic proteins were also observed in thymus from ADR-treated mice.[30] Alterations to metabolism in

peripheral immune organs (i.e., spleen, and thymus) can be compared with reports describing changes to myocardial energy metabolism.[67] Differential expression of metabolic splenic proteins shows that ADR treatment has downstream effects in glycolysis, glucogenesis, and other metabolic pathways. For example, aldose reductase which converts glucose to fructose during impaired glycolysis also functions to reduce toxicity of lipid peroxidation products such as 4-hydroxy-trans-nonenal. Down-regulation of this particular enzyme may be detrimental to spleen in ADR-treated mice. Normal energy production is critical to help cells have a better defense response against cellular toxicity and cancer and to maintain normal cellular homeostasis.

Redox/Cellular Signaling/Transport

The redox system in the cell is crucial to maintaining a balance between reactive oxygen species and antioxidants which keeps cells free from oxidative stress and damage. Redox processes are differentially altered following ADR treatment in cancer cells.[31] Splenic proteins involved in cellular signaling and transport processes were differentially regulated in ADR-treated mice (Table 2) and have been implicated in other proteomic studies investigating effects of ADR treatment.[22,27−29] Peptidyl-prolyl cis−trans isomerase B belongs to the family of PPIase enzymes that isomerize proline residues in target proteins and assist in protein folding. This particular PPIase is upregulated in spleen, whereas Pin 1 is downregulated in the brains of ADR-treated mice.[22] Myosin proteins (i.e., myosin, myosin-11, myosin-9) are ATP-dependent proteins which regulate actin-based cell motility and were detected as upregulated in these studies. Myosin-9 and myosin-11 were downregulated in mitochondrial Raji cells after ADR treatment.[29] The differences observed in expression of myosin, Pin1, and 14-3-3 may be tissue specific. Upregulation of these proteins following ADR treatment could be related to upregulation of cytoskeletal proteins, which would be necessary for maintenance of cellular structure and hence cellular transport.

CONCLUSIONS

ADR treatment has been reported to have detrimental effects on a number of tissues in animal models and in cell cultures. This work reported on the downstream effects of ADR-treatment on spleen tissue in mice. These effects include reduced spleen size and alterations to the global splenic proteome for proteins involved in cellular processes such as cystokeletal structural integrity, Ca^{2+} binding, immune response, and others. It is possible that ADR treatment through alterations to protein expression lead to weakened immunity. Insights gained from these studies will be useful for understanding toxic mechanisms of ADR treatment which is necessary to minimize drug side effects and improve quality of life in cancer patients undergoing ADR treatment.

ASSOCIATED CONTENT

Supporting Information

Table listing all peptides used for quantitation for identified proteins. This material is available free of charge via the Internet at http://pubs.acs.org.

AUTHOR INFORMATION

Corresponding Author

*Mailing address: Department of Chemistry, University of Pittsburgh , 111 Eberly Hall, 200 University Drive, Pittsburgh, PA 15260, USA. Telephone: +1-412-624-8167. Fax: +1-412-624-8611. E-mail: rena@pitt.edu.

ACKNOWLEDGMENT

The authors acknowledge the University of Kentucky Markey Cancer Center and the University of Pittsburgh for funds to support this work.

REFERENCES

(1) Bonadonna, G. Perspectives in Cancer Research - Articles Evolving Concepts in the Systemic Adjuvant Treatment of Breast Cancer. *Cancer Res.* **1992**, *52*, 2127–2137.

(2) Di Marco, A. G., M; Scarpinato, B. Adriamycin (NCS-123, 127): a new antibiotic with antitumor activity. *Cancer Chemother. Rep.* **1969**, *53* (1), 33–37.

(3) Chuang, R. Y.; Chuang, L. F. Inhibition of chicken myeloblastosis RNA polymerase II activity by adriamycin. *Biochemistry* **1979**, *18* (10), 2069–2073.

(4) Cummings, J.; Anderson, L.; Willmott, N.; Smyth, J. F. The molecular pharmacology of doxorubicin in vivo. *Eur. J. Cancer* **1991**, *27* (5), 532–535.

(5) Buzdar, A. U.; Marcus, C.; Smith, T. L.; Blumenschein, G. R. Early and delayed clinical cardiotoxicity of doxorubicin. *Cancer* **1985**, *55* (12), 2761–2765.

(6) Aluise, C. D.; Sultana, R.; Tangpong, J.; Vore, M.; St Clair, D.; Moscow, J. A.; Butterfield, D. A. Chemo brain (chemo fog) as a potential side effect of doxorubicin administration: role of cytokine-induced, oxidative/nitrosative stress in cognitive dysfunction. *Adv. Exp. Med. Biol.* **2010**, *678*, 147–156.

(7) Schagen, S. B.; Hamburger, H. L.; Muller, M. J.; Boogerd, W.; van Dam, F. S. Neurophysiological evaluation of late effects of adjuvant high-dose chemotherapy on cognitive function. *J. Neurooncol.* **2001**, *51* (2), 159–165.

(8) Multani, P.; White, C. A.; Grillo-Lopez, A. Non-Hodgkin's lymphoma: review of conventional treatments. *Curr. Pharm. Biotechnol.* **2001**, *2* (4), 279–291.

(9) Handa, K.; Sato, S. Generation of free radicals of quinone group-containing anti-cancer chemicals in NADPH-microsome system as evidenced by initiation of sulfite oxidation. *Gann* **1975**, *66* (1), 43–47.

(10) Chen, Y.; Jungsuwadee, P.; Vore, M.; Butterfield, D. A.; St Clair, D. K. Collateral damage in cancer chemotherapy: oxidative stress in nontargeted tissues. *Mol. Interventions* **2007**, *7* (3), 147–156.

(11) Aluise, C. D.; St Clair, D.; Vore, M.; Butterfield, D. A. In vivo amelioration of adriamycin induced oxidative stress in plasma by gamma-glutamylcysteine ethyl ester (GCEE). *Cancer Lett.* **2009**, *282* (1), 25–29.

(12) Joshi, G.; Sultana, R.; Tangpong, J.; Cole, M. P.; St Clair, D. K.; Vore, M.; Estus, S.; Butterfield, D. A. Free radical mediated oxidative stress and toxic side effects in brain induced by the anti cancer drug adriamycin: insight into chemobrain. *Free Radical Res.* **2005**, *39* (11), 1147–1154.

(13) Llesuy, S. F.; Milei, J.; Gonzalez Flecha, B. S.; Boveris, A. Myocardial damage induced by doxorubicins: hydroperoxide-initiated chemiluminescence and morphology. *Free Radical Biol. Med.* **1990**, *8* (3), 259–264.

(14) DeAtley, S. M.; Aksenov, M. Y.; Aksenova, M. V.; Carney, J. M.; Butterfield, D. A. Adriamycin induces protein oxidation in erythrocyte membranes. *Pharmacol. Toxicol.* **1998**, *83* (2), 62–68.

(15) Qin, X. J.; He, W.; Hai, C. X.; Liang, X.; Liu, R. Protection of multiple antioxidants Chinese herbal medicine on the oxidative stress induced by adriamycin chemotherapy. *J. Appl. Toxicol.* **2008**, *28* (3), 271–282.

(16) Prahalathan, C.; Selvakumar, E.; Varalakshmi, P. Remedial effect of DL-alpha-lipoic acid against adriamycin induced testicular lipid peroxidation. *Mol. Cell. Biochem.* **2004**, *267* (1−2), 209–214.

(17) Kalaiselvi, P.; Pragasam, V.; Chinnikrishnan, S.; Veena, C. K.; Sundarapandiyan, R.; Varalakshmi, P. Counteracting adriamycin-induced oxidative stress by administration of N-acetyl cysteine and vitamin E. *Clin. Chem. Lab. Med.* **2005**, *43* (8), 834–840.

(18) Green, P. S.; Leeuwenburgh, C. Mitochondrial dysfunction is an early indicator of doxorubicin-induced apoptosis. *Biochim. Biophys. Acta* **2002**, *1588* (1), 94–101.

(19) Siegfried, J. A.; Kennedy, K. A.; Sartorelli, A. C.; Tritton, T. R. The role of membranes in the mechanism of action of the antineoplastic agent adriamycin. Spin-labeling studies with chronically hypoxic and drug-resistant tumor cells. *J. Biol. Chem.* **1983**, *258* (1), 339–343.

(20) Kusuoka, H.; Futaki, S.; Koretsune, Y.; Kitabatake, A.; Suga, H.; Kamada, T.; Inoue, M. Alterations of intracellular calcium homeostasis and myocardial energetics in acute adriamycin-induced heart failure. *J. Cardiovasc. Pharmacol.* **1991**, *18* (3), 437–444.

(21) Singh, V.; Singh, S. M. Effect of high cell density on the growth properties of tumor cells: a role in tumor cytotoxicity of chemotherapeutic drugs. *Anticancer Drugs* **2007**, *18* (10), 1123–1132.

(22) Joshi, G.; Aluise, C. D.; Cole, M. P.; Sultana, R.; Pierce, W. M.; Vore, M.; St Clair, D. K.; Butterfield, D. A. Alterations in brain antioxidant enzymes and redox proteomic identification of oxidized brain proteins induced by the anti-cancer drug adriamycin: implications for oxidative stress-mediated chemobrain. *Neuroscience* **2010**, *166* (3), 796–807.

(23) Joshi, G.; Hardas, S.; Sultana, R.; St Clair, D. K.; Vore, M.; Butterfield, D. A. Glutathione elevation by gamma-glutamyl cysteine ethyl ester as a potential therapeutic strategy for preventing oxidative stress in brain mediated by in vivo administration of adriamycin: Implication for chemobrain. *J. Neurosci. Res.* **2007**, *85* (3), 497–503.

(24) Aluise, C. D.; Miriyala, S.; Noel, T.; Sultana, R.; Jungsuwadee, P.; Taylor, T. J.; Cai, J.; Pierce, W. M.; Vore, M.; Moscow, J. A.; St Clair, D. K.; Butterfield, D. A. 2-Mercaptoethane sulfonate prevents doxorubicin-induced plasma protein oxidation and TNF-alpha release: implications for the reactive oxygen species-mediated mechanisms of chemobrain. *Free Radical Biol. Med.* **2011**, *50* (11), 1630–1638.

(25) Chen, Y.; Daosukho, C.; Opii, W. O.; Turner, D. M.; Pierce, W. M.; Klein, J. B.; Vore, M.; Butterfield, D. A.; St Clair, D. K. Redox proteomic identification of oxidized cardiac proteins in adriamycin-treated mice. *Free Radical Biol. Med.* **2006**, *41* (9), 1470–1477.

(26) Chen, S. T.; Pan, T. L.; Tsai, Y. C.; Huang, C. M. Proteomics reveals protein profile changes in doxorubicin-treated MCF-7 human breast cancer cells. *Cancer Lett.* **2002**, *181* (1), 95–107.

(27) Hammer, E.; Bien, S.; Salazar, M. G.; Steil, L.; Scharf, C.; Hildebrandt, P.; Schroeder, H. W.; Kroemer, H. K.; Volker, U.; Ritter, C. A. Proteomic analysis of doxorubicin-induced changes in the proteome of HepG2cells combining 2-D DIGE and LC-MS/MS approaches. *Proteomics* **2010**, *10* (1), 99–114.

(28) Dong, X.; Xiong, L.; Jiang, X.; Wang, Y. Quantitative proteomic analysis reveals the perturbation of multiple cellular pathways in jurkat-T cells induced by doxorubicin. *J. Proteome Res.* **2010**, *9* (11), 5943–5951.

(29) Jiang, Y. J.; Sun, Q.; Fang, X. S.; Wang, X. Comparative mitochondrial proteomic analysis of Rji cells exposed to adriamycin. *Mol. Med.* **2009**, *15* (5−6), 173–182.

(30) Sultana, R.; Di Domenico, F.; Tseng, M.; Cai, J.; Noel, T.; Chelvarajan, R. L.; Pierce, W. D.; Cini, C.; Bondada, S.; St Clair, D. K.; Butterfield, D. A. Doxorubicin-induced thymus senescence. *J. Proteome Res.* **2010**, *9* (12), 6232–6341.

(31) Zhang, J.-T.; Liu, Y. Use of Comparative Proteomics to Identify Potential resistance Mechanisms in Cancer Treatment. *Cancer Treatment Rev.* **2007**, *33*, 741–756.

(32) Peng, X.; Gong, F.; Xie, G.; Zhao, Y.; Tang, M.; Yu, L.; Tong, A. A proteomic investigation into adriamycin chemo-resistance of human leukemia K562 cells. *Mol. Cell. Biochem.* **2011**, *351* (1−2), 233–241.

(33) Shen, S. H.; Gu, L. J.; Liu, P. Q.; Ye, X.; Chang, W. S.; Li, B. S. Comparative proteomic analysis of differentially expressed proteins between K562 and K562/ADM cells. *Chin. Med. J. (Engl.)* **2008**, *121* (5), 463–468.

(34) Zhu, F.; Wang, Y.; Zeng, S.; Fu, X.; Wang, L.; Cao, J. Involvement of annexin A1 in multidrug resistance of K562/ADR cells identified by the proteomic study. *OMICS* **2009**, *13* (6), 467–476.

(35) Keenan, J.; Murphy, L.; Henry, M.; Meleady, P.; Clynes, M. Proteomic analysis of multidrug-resistance mechanisms in adriamycin-resistant variants of DLKP, a squamous lung cancer cell line. *Proteomics* **2009**, *9* (6), 1556–1566.

(36) Brown, K. J.; Fenselau, C. Investigation of doxorubicin resistance in MCF-7 breast cancer cells using shot-gun comparative proteomics with proteolytic 18O labeling. *J. Proteome Res.* **2004**, *3* (3), 455–462.

(37) Gehrmann, M. L.; Fenselau, C.; Hathout, Y. Highly altered protein expression profile in the adriamycin resistant MCF-7 cell line. *J. Proteome Res.* **2004**, *3* (3), 403–409.

(38) Strong, R.; Nakanishi, T.; Ross, D.; Fenselau, C. Alterations in the mitochondrial proteome of adriamycin resistant MCF-7 breast cancer cells. *J. Proteome Res.* **2006**, *5* (9), 2389–2395.

(39) Gehrmann, M. L.; Hathout, Y.; Fenselau, C. Evaluation of metabolic labeling for comparative proteomics in breast cancer cells. *J. Proteome Res.* **2004**, *3* (5), 1063–1068.

(40) Orsini, F.; Pavelic, Z.; Mihich, E. Increased primary cell-mediated immunity in culture subsequent to adriamycin or daunorubicin treatment of spleen donor mice. *Cancer Res.* **1977**, *37* (6), 1719–1726.

(41) Chakraborty, A.; Regnier, F. E. Global internal standard technology for comparative proteomics. *J. Chromatogr., A* **2002**, *949* (1−2), 173–184.

(42) Ji, J.; Chakraborty, A.; Geng, M.; Zhang, X.; Amini, A.; Bina, M.; Regnier, F. Strategy for qualitative and quantitative analysis in proteomics based on signature peptides. *J. Chromatogr., B: Biomed. Sci. Appl.* **2000**, *745* (1), 197–210.

(43) Mebius, R. E.; Kraal, G. Structure and function of the spleen. *Nat. Rev. Immunol.* **2005**, *5* (8), 606–616.

(44) Lee, J. W.; Sung, N. Y.; Kim, J. K.; Kim, J. H.; Raghavendran, H. R.; Yoo, Y. C.; Shin, M. H.; Byun, M. W. Effect of gamma irradiation on spleen cell function and cytotoxicity of doxorubicin. *Chem.-Biol. Interact.* **2008**, *173* (3), 205–214.

(45) Miranda, C. J.; Makui, H.; Soares, R. J.; Bilodeau, M.; Mui, J.; Vali, H.; Bertrand, R.; Andrews, N. C.; Santos, M. M. Hfe deficiency increases susceptibility to cardiotoxicity and exacerbates changes in iron metabolism induced by doxorubicin. *Blood* **2003**, *102* (7), 2574–2580.

(46) Wu, W. R.; Zheng, J. W.; Li, N.; Bai, H. Q.; Zhang, K. R.; Li, Y. Immunosuppressive effects of dihydroetorphine, a potent narcotic analgesic, in dihydroetorphine-dependent mice. *Eur. J. Pharmacol.* **1999**, *366* (2−3), 261–269.

(47) Zhang, X. Y.; Li, W. G.; Wu, Y. J.; Zheng, T. Z.; Li, W.; Qu, S. Y.; Liu, N. F. Proanthocyanidin from grape seeds potentiates anti-tumor activity of doxorubicin via immunomodulatory mechanism. *Int. Immunopharmacol.* **2005**, *5* (7−8), 1247–1257.

(48) Cesta, M. F. Normal structure, function, and histology of the spleen. *Toxicol. Pathol.* **2006**, *34* (5), 455–465.

(49) Gerke, V.; Moss, S. E. Annexins: from structure to function. *Physiol. Rev.* **2002**, *82* (2), 331–371.

(50) Zhang, F.; Zhang, L.; Zhang, B.; Wei, X.; Yang, Y.; Qi, R. Z.; Ying, G.; Zhang, N.; Niu, R. Anxa2 plays a critical role in enhanced invasiveness of the multidrug resistant human breast cancer cells. *J. Proteome Res.* **2009**, *8* (11), 5041–5047.

(51) Munoz, L. E.; Frey, B.; Pausch, F.; Baum, W.; Mueller, R. B.; Brachvogel, B.; Poschl, E.; Rodel, F.; von der Mark, K.; Herrmann, M.; Gaipl, U. S. The role of annexin A5 in the modulation of the immune response against dying and dead cells. *Curr. Med. Chem.* **2007**, *14* (3), 271–277.

(52) Gelebart, P.; Opas, M.; Michalak, M. Calreticulin, a Ca2+-binding chaperone of the endoplasmic reticulum. *Int. J. Biochem. Cell Biol.* **2005**, *37* (2), 260–266.

(53) Gold, L. I.; Eggleton, P.; Sweetwyne, M. T.; Van Duyn, L. B.; Greives, M. R.; Naylor, S. M.; Michalak, M.; Murphy-Ullrich, J. E. Calreticulin: non-endoplasmic reticulum functions in physiology and disease. *FASEB J.* **2010**, *24* (3), 665–683.

(54) Tufi, R.; Panaretakis, T.; Bianchi, K.; Criollo, A.; Fazi, B.; Di Sano, F.; Tesniere, A.; Kepp, O.; Paterlini-Brechot, P.; Zitvogel, L.; Piacentini, M.; Szabadkai, G.; Kroemer, G. Reduction of endoplasmic reticulum Ca2+ levels favors plasma membrane surface exposure of calreticulin. *Cell Death Differ.* **2008**, *15* (2), 274–282.

(55) Mayur, Y. C.; Jagadeesh, S.; Thimmaiah, K. N. Targeting calmodulin in reversing multi drug resistance in cancer cells. *Mini-Rev. Med. Chem.* **2006**, *6* (12), 1383–1389.

(56) Nicotera, P.; Bellomo, G.; Orrenius, S. Calcium-mediated mechanisms in chemically induced cell death. *Annu. Rev. Pharmacol. Toxicol.* **1992**, *32*, 449–470.

(57) Storck, S.; Shukla, M.; Dimitrov, S.; Bouvet, P. Functions of the histone chaperone nucleolin in diseases. *Subcell. Biochem.* **2007**, *41*, 125–144.

(58) Bonello, T. T.; Stehn, J. R.; Gunning, P. W. New approaches to targeting the actin cytoskeleton for chemotherapy. *Future Med. Chem.* **2009**, *1* (7), 1311–1331.

(59) Oikonomou, K. G.; Zachou, K.; Dalekos, G. N. Alpha-actinin: a multidisciplinary protein with important role in B-cell driven autoimmunity. *Autoimmun. Rev.* **2011**, *10* (7), 389–396.

(60) Yang, Y. X.; Sun, X. F.; Cheng, A. L.; Zhang, G. Y.; Yi, H.; Sun, Y.; Hu, H. D.; Hu, P.; Ye, F.; Chen, Z. C.; Xiao, Z. Q. Increased expression of HSP27 linked to vincristine resistance in human gastric cancer cell line. *J. Cancer Res. Clin. Oncol.* **2009**, *135* (2), 181–189.

(61) Zhang, L. H.; Zhang, X. Roles of GRP78 in physiology and cancer. *J. Cell. Biochem.* **2010**, *110* (6), 1299–1305.

(62) Kubota, H.; Hynes, G.; Willison, K. The chaperonin containing t-complex polypeptide 1 (TCP-1). Multisubunit machinery assisting in protein folding and assembly in the eukaryotic cytosol. *Eur. J. Biochem.* **1995**, *230* (1), 3–16.

(63) Kazerounian, S.; Yee, K. O.; Lawler, J. Thrombospondins in cancer. *Cell. Mol. Life Sci.* **2008**, *65* (5), 700–712.

(64) Piccard, H.; Van den Steen, P. E.; Opdenakker, G. Hemopexin domains as multifunctional liganding modules in matrix metalloproteinases and other proteins. *J. Leukocyte Biol.* **2007**, *81* (4), 870–892.

(65) Hempel, N.; Carrico, P. M.; Melendez, J. A. Manganese superoxide dismutase (Sod2) and redox-control of signaling events that drive metastasis. *Anticancer Agents Med. Chem.* **2011**, *11* (2), 191–201.

(66) Yen, H. C.; Oberley, T. D.; Vichitbandha, S.; Ho, Y. S.; St Clair, D. K. The protective role of manganese superoxide dismutase against adriamycin-induced acute cardiac toxicity in transgenic mice. *J. Clin. Invest.* **1996**, *98* (5), 1253–1260.

(67) Tokarska-Schlattner, M.; Wallimann, T.; Schlattner, U. Alterations in myocardial energy metabolism induced by the anti-cancer drug doxorubicin. *C. R. Biol.* **2006**, *329* (9), 657–668.